



Journal of Food Science and Technology (Iran)

Homepage: www.fsct.modares.ir

Scientific Research

Investigating the properties of barija gum oleoresin extracted by the method of deep eutectic solvents

Javad Radmard ¹, Ali Mohammadi Sanni Kakhki ², Akram Arianfar ², Behrooz Mahmoodzadeh Vaziri ^{3,4}

1- Ph.D student, Department of Food Science and Technology, Qu.C., Islamic Azad University, Quchan, Iran

2- Department of Food Science and Technology, Qu.C., Islamic Azad University, Quchan, Iran

3- Department of Chemical engineering, Qu.C., Islamic Azad University, Quchan, Iran

4- Department of Chemical Engineering, Ma.C., Islamic Azad University, Mashhad, Iran

ARTICLE INFO

ABSTRACT

Article History:

Received: 2023/10/04

Accepted: 2024/04/23

Keywords:

Extraction,
Oleoresin,
Barijeh, functional-structural
properties.

DOI: 10.48311/fsct.2025.83974.0.

*Corresponding Author E-

Mohamadisani@yahoo.com

Deep eutectic solvents have found many advantages in the extraction of plant metabolites, such as low toxicity, biodegradability, low cost, and ease of preparation compared to conventional methods. The aim of this work is to compare the natural deep eutectic solvents in the extraction of *Ferula gummosa* (Ferula gummosa) and determine its chemical, structural, thermal and rheological properties. Six eutectic solvent mixtures including choline chloride/urea, acetic acid, lactic acid, formic acid, formamide and glycerol in ratios of 2:1 and 3:1 were evaluated. The highest yield was obtained for choline chloride/formic acid, choline chloride/formamide. The main components of oleoresin were β -pinene (40.27%), silcophenone (11.93%) and α -pinene (7.53%), which were determined by gas chromatography-mass spectrometry. Gum was mainly composed of carbohydrates (67.39% by weight). The polysaccharide consisted of a main backbone of (1 \rightarrow 3)- β -D-galactan branched mainly from O-6 but also from O-4 and O-4,6. The X-ray diffraction pattern showed a semi-crystalline microstructure. The thermal behavior of the gum was evaluated by thermal analysis (TGA) and differential scanning calorimetry (DSC) showed temperatures below and above 200 °C as the dominant weight loss regions. The rheological behavior of oleoresin was non-Newtonian behavior of shear thinning type, which was well fitted by the power law model. Studying the chemical structure by spectrometry showed that no solvent remained in oleoresin. Therefore, barijeh oleoresin can be used as a promising natural medicinal substance extracted with eutectic solvents, while these eutectic solvents can be used as a green method for many herbal compounds.

1. Introduction

The plant Barijeh (*ferula gummosa Boiss*) belonging to the subfamily Apioidae is a wild herbaceous plant native to Iran. It is a perennial plant with a height of approximately 3 to 8 meters that can live for about 6 to 8 years. The plant produces a strong-smelling resin naturally excreted by seeds at temperatures below 5 degrees Celsius in mountainous regions in the north and west of the country at altitudes of 1800 to 3000 meters above sea level with an average rainfall of 250 to 500 millimeters per year. Barijeh has a glandular root rich in Oleoresin, and this resinous substance is usually referred to as galbanum. The average production of galbanum is around 10 grams per bush, and by following proper harvesting methods, maximum Oleoresin production can be achieved without harming the plant. Galbanum derived from Barijeh is known for its bioactive properties such as antimicrobial, anticonvulsant, anti-flatulence, mucolytic, stimulant, diuretic, anti-rheumatic, analgesic, anti-hysterical, laxative, aphrodisiac, anti-infective, anti-diabetic properties as well as multiple medicinal applications. Additionally, Barijeh's Oleoresin is used in the manufacture of adhesive tapes, textiles, cosmetics, gem adhesives, and jewelry glue due to its transparency and high bonding strength.

The chemical composition of essential oils from different species of Barijeh has been studied, and the main components of Barijeh include alpha-pinene, beta-pinene, alpha-thuyene, camphene, beta-phellandrene, and sabinene, which collectively constitute about 82% of the oily fraction. The Oleoresin extraction yield is reported to be 6.10%, with the main components being beta-pinene (58.8%), camphor (12.1%), alpha-pinene (7.5%), and beta-myrcene (6.4%). Furthermore, 73 monoterpenes have been identified in the essential oil extract of Barijeh fruit using liquid gas chromatography, among which alpha-pinene and beta-pinene, along with myrcene, are the main components, constituting about 73% of the oil fraction. In another study, the chemical composition of Barijeh's Oleoresin has been reported to include monoterpenoid hydrocarbons (88%), including sabinene, alpha-pinene, and beta-pinene.

Given the wide range of aforementioned applications, galbanum is one of Iran's most important exportable herbal products. Therefore, the precise identification of this

natural source is of great importance. This knowledge enables more effective quality control for current applications, thereby preventing fraud. It also opens up new opportunities for utilizing it with high added value.

The extraction, separation, or purification of bio-molecular extracts rich in pure plant compounds is crucial. Extraction, as the most important stage, typically involves the use of organic solvents with high extraction capacity. However, most organic solvents are flammable, toxic, and biodegradation-resistant, thus not meeting the green chemistry-friendly environment-growing trend. Supercritical fluids or biobased solvents (such as ethanol, limonene, ethyl lactate, glycerol, or 2-methyltetrahydrofuran) can serve as alternatives, but they can only provide a limited solution for certain applications. In the early 2000s, a new type of solvents called "Deep Eutectic Solvents" (DES) emerged. The increasing demand for environmentally friendly processes within the framework of green and sustainable chemistry, along with the notable properties and benefits of DES in the past two decades, has led to a growing use of these mixtures as alternative solvents to conventional solvents and ionic liquids in various fields. Although DESs are somewhat similar to ionic liquids, they are cheaper, easily and quickly synthesized with low energy, and most are biodegradable with low toxicity. Therefore, numerous studies have been published on the synthesis, properties, and applications of DES.

Deep Eutectic Solvents are mixtures of two or more solvents that show a significant reduction in the melting point at a specific composition and turn into a liquid at room temperature. The constituents of DES are primary metabolites such as sugars (glucose, sucrose, and fructose), organic acids (lactic, malic, and citric acids), urea, and quaternary ammonium salts (choline chloride or betaine). DESs have been used in the extraction of common metabolites, polar and non-polar compounds from plants such as green coffee beans, *seudowintera colorata*, ginkgo biloba, mangosteen pericarp, sage, olive, citrus grandis L. Osbeck, *Herba Artemisiae Scopariae*, *Cynara cardunculus*, *Carthamus tinctorius*, black wheat bran, fig leaves, *Sophora japonica*, and *Cajanus cajan*. Despite the numerous studies conducted on the extraction of various bioactive compounds such

as anthocyanins, polyphenols, flavonoids, and catechins using DES, unfortunately, there has been no research on the extraction of Oleoresin from Barijeh resin using Deep Eutectic Solvents and investigating its structural and functional properties. Therefore, the aim of this

2. Materials and Methods

2.1. Materials

The Barijeh plant roots were collected in September 2021 at an altitude of approximately 2340 meters above sea level from the city of Farooj. A sample was sent to the Herbarium of the Forests and Rangelands Research Institute (TARI), Tehran, Iran for identification and confirmation. Following previous work by Jalali, soil around the lower part of the plant stem was harvested, and the surface near the roots was scratched to collect exudates for one week in a stainless steel container. Oleoresin was obtained from approximately 100 healthy 4-6 years old plants. The mixed exudates were stored in a tightly sealed plastic container in a refrigerator (4 degrees Celsius). Deep Eutectic Solvents (DES) including choline chloride (CL) (purity 99%) as the HBA, and urea (purity 99-100%), lactic acid (purity >85%), acetic acid (purity >85%), formic acid (purity >85%), and glycerol (purity >90%) as the HBDs were obtained from Merck (Darmstadt, Germany).

2-2- Synthesis of deep eutectic solvents

The deep eutectic solvent was prepared with slight modifications based on previous works [37]. Solutions of CL-urea, CL-acetic acid, CL-lactic acid, and CL-glycerol were prepared in a ratio of 2:1, whereas CL-formic acid and CL-formamide were obtained in a 3:1 ratio. The molar ratio of DES was chosen based on initial experiments. Choline chloride (HBA) and other solvents such as HBD were separately mixed at an optimal molar ratio in a reactor heated to 90 degrees Celsius for 4 hours using a magnetic stirrer at 400 revolutions per minute to obtain a clear liquid. The DES was stored in a glass vial with a screw cap under dark conditions. DES samples were periodically inspected over several weeks for crystal formation.

2-3- Oleoresin extraction from Barijeh

Oleoresin was extracted from the exudates using water distillation in a Clevenger apparatus for 3 hours and recovered with diethyl ether. It was then dried over anhydrous sodium sulfate and carefully evaporated with a

research is to utilize suitable DES for the extraction of Oleoresin from Barijeh resin, compare it with the conventional method, and ultimately study the practical properties of this resin.

rotary evaporator. The Oleoresin was stored at 4 degrees Celsius until further analysis.

Six DES mixtures were used separately for Oleoresin extraction from Barijeh. In a typical experiment, 1000 milligrams of Barijeh exudates were separately mixed with 5 grams of DES in a beaker. The mixture was then heated at temperatures between 30-50 degrees Celsius for various time periods (3, 6, and 9 hours). After centrifugation at 3000 revolutions per minute for 5 minutes, the obtained mass at the bottom of the centrifuge tube was separated, washed with IPA several times, and dried under vacuum. In a control experiment, 500 milligrams of Barijeh exudates were mixed with 10 milliliters of ethanol, and the temperature and time were maintained similar to previous reactions. The resulting liquid was precipitated with ethanol, and the precipitated Oleoresin was dried under vacuum.

2-4- Gas chromatography analysis

Gas chromatography-mass spectrometry (GC-MS) analysis was performed using a gas chromatograph (7890B, Agilent, Santa Clara, CA, USA) connected to a mass spectrometer (5977A, Agilent Technologies, USA). The gas chromatograph was equipped with an HP-5 capillary column (phenyl methyl siloxane, 30 meters length, 0.25 mm inner diameter, and 0.25 μ m film thickness, Agilent). The injector temperature was set at 270 degrees Celsius, and the oven temperature was programmed from 60 to 200 degrees Celsius at a rate of 5 degrees Celsius per minute. Helium was used as the carrier gas with a flow rate of 1 milliliter per minute, and an injection volume of 1 microliter was set. The mass spectrometer was tuned to electron ionization mode at 70 electron volts. The surface temperature was set at 280 degrees Celsius, and the mass range was set between 35 to 500 m/z. The components of Oleoresin were identified based on the comparison of their retention indices (C7 to C20 n-alkanes) and the fragmentation patterns from the gas chromatography-mass spectrometry analysis using Kovats indices equations.

2-5- Structural analysis

Fourier-transform infrared (FTIR) spectroscopy of Oleoresin was conducted using a Perkin-Elmer FTIR spectrometer (Spectrum GX, USA). Measurements were taken in the range of 400 to 4000 cm^{-1} with 50 scans and a resolution of 1 cm^{-1} , as per previous work with some modifications.

2-6- NMR spectroscopy

Oleoresin from Barijeh was dissolved in deuterated water (D_2O) at a concentration of 99%, and frozen to replace exchangeable protons with deuterium. Prior to NMR analysis, Oleoresin was dissolved in D_2O (50g per liter). One and two-dimensional NMR spectra were recorded on a Bruker Advance 400 spectrometer (Germany) at frequencies of 400 MHz (64 scans) for ^1H and 100 MHz (8192 scans) for ^{13}C . NMR experiments including ^1H , ^{13}C , heteronuclear, and multiple quantum coherence were carried out at 30 degrees Celsius. All chemical shifts were referenced to Me_4Si .

2-7- X-ray diffraction

X-ray diffraction analysis was performed using an XRD-6000 diffractometer operating at 40 kV and 40 mA, with $\text{Cu K}\alpha$ radiation in the 2θ range of 10 – 100° with a step size of 0.06684° . The crystallinity index was calculated based on the equation proposed by Petersen (1939) using the Origin software.

2-8- Thermal analysis

Thermogravimetric analysis (TGA) was performed using a TA instrument (TGA 2050, USA). One gram of Oleoresin was placed on an aluminum pan and heated from 50 to 500 degrees Celsius under a nitrogen atmosphere. The weight loss difference was reported for thermal stability calculation.

The TA instrument (DSC Q2000, USA) was used to analyze the thermal behavior of Barijeh resin. A 14-milligram sample was placed in an aluminum crucible, and the heating process involved a temperature range of 50 to 400 degrees Celsius at a rate of 10 degrees per minute under a nitrogen atmosphere. Data was obtained using the instrument software.

2-9- Rheological behavior analysis

The flow behavior and apparent viscosity of the samples were examined using a Brookfield rotational viscometer (Model DV-III Ultra, USA). Measurements were taken with a SC4-

18 spindle at a temperature of 20 degrees Celsius and shear rates between 300-10 per second. Modeling of the Oleoresin flow behavior was carried out using the power law model and Sigma Plot software version 7.

2-10- Statistical analysis

Data were presented as mean \pm standard deviation. Experimental design and regression analysis were conducted using Sigma Plot software version 7. Statistical analysis was performed with Origin 8.0, and statistical significance was determined at $p < 0.05$. The proposed model fit was assessed by evaluating the coefficient of determination (R^2), lack of fit, and F-value using analysis of variance (ANOVA).

3. Results and discussion

3.1. Selection of Deep Eutectic Solvent Type

As mentioned earlier, DESs have been widely used for the extraction of antioxidants, polyphenols, and many polar compounds from plant materials. In the current study, six types of DES were utilized for the extraction of Oleoresin from Barijeh (Table 1). The results showed that the efficiency of Oleoresin extraction was higher when using the CL/formic acid and CL/formamide solvents, which may be attributed to the stronger hydrogen bonding capability of DESs created by choline chloride and formic acid or formamide. This could lead to a strong intermolecular bond with Oleoresin in *Ferula gummosa* [42]. However, when the molar ratio of CL/formic acid and CL/formamide solvents changed from 2:1 to 3:1, the extraction efficiency increased. These results can be attributed to the acidic hydrolysis of intercellular wall bonds due to the acidic properties of formic acid in the DES (i.e., a higher amount of formic acid present in the DES), which released Oleoresin freely in the extraction medium and increased the efficiency. The extraction efficiency was consistent with previous findings [43]. An increase in the molar ratio of choline chloride led to a decrease in the extraction rate of Oleoresin, as an increase in the CL ratio resulted in an increase in the solvent's pH, thus affecting the performance of Oleoresin. Therefore, the highest extraction of Oleoresin was achieved with the specified ratios shown in Table 1. Consequently, the DES solvent composed of CL/formic acid and CL/formamide was chosen for further research.

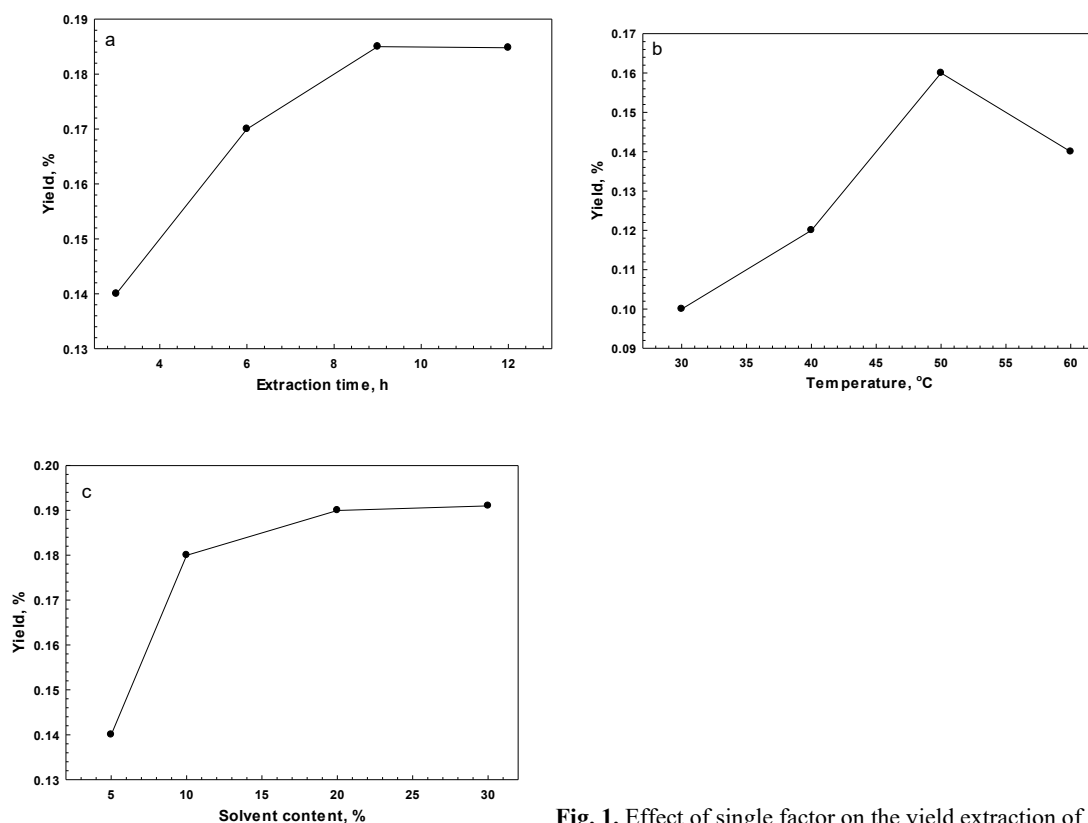
Table 1. *F. gummsa* oleoresin yields corresponding to different DES solvents.

HBA: HBD	Molar ratio	Oleoresin yield (%)
CL: Urea	2:1	13.62 ± 0.94
CL: Lactic acid	2:1	13.28 ± 0.78
CL: Formic acid	3:1	15.37 ± 1.16
CL: Acetic acid	2:1	13.83 ± 1.14
CL: Glycerol	2:1	11.61 ± 0.61
CL: Formamide	3:1	15.68 ± 1.25

3.2. Effect of factors on the Oleoresin extraction

The effect of time, temperature, and the ratio of DES solvent to *F. gummsa* on the extraction yield of ellorozine is shown in Figure 1. As observed, the extraction yield increased with time and temperature. However, higher temperatures and longer periods were not used due to changes in the physical properties of the DES. The results showed that with an increase in extraction time from 3 to 9 hours, the ellorozine yield significantly increased ($P < 0.05$) and the maximum yield (67.18%) was obtained at 9 hours (Figure 1a), which is due to the time (3 hours) required for complete release of ellorozine in the extraction medium. During

the process, the DES solution penetrated the *F. gummsa* matrices, hydrolyzed the dissolved cell wall linkages, and then released outside the cell wall. However, when the extraction time increased to 10 hours, no further increase in performance was observed. When the temperature increased from 30 to 50 degrees Celsius, the performance significantly increased from 2.9 to 4.17% ($P < 0.05$) (Figure 1b). This increase in performance with temperature increase was associated with an increase in ellorozine permeability. The temperature increase reduced the diffusion viscosity of DES, which helped break the chemical bond between ellorozine and the cell wall, thus improving ellorozine dissolution. During extraction, heat increased the breakage of bonds between cell walls. Similar results have been found in the extraction of polysaccharides from blackberries, where an increase in extraction temperature from 60 to 90 degrees Celsius led to improved performance. As shown in Figure 1c, when the ratio of DES solvent to *F. gummsa* exceeded 20%, the extraction yield decreased, while at 10%, the ellorozine yield reached a maximum of 18%.

**Fig. 1.** Effect of single factor on the yield extraction of oleoresin.

(a) Extraction time (h), (b) Extraction temperature (°C), and (c) solvent content(%).

3.3. Chemical compounds of Oleoresin

The results of GC-MS analysis of *F.gummosa* oleoresin are shown in Table 2. Compounds are ranked in order of retention time. A total of 20 compounds were identified in oleoresin, with β -pinene (40.27%), silcofenchenes (11.93%), and α -pinene (7.53%) being the main components. The main group of monoterpene hydrocarbons (62.70%) included α -thogen, α -pinene and β -pinene. Other main components of oleoresin were β -cymene (8.2%) and α -thogen (10.49%). The results showed that the monoterpene component constitutes 60% of the oil components and terpenes are the remaining

components (~40%), which is consistent with previous studies [6]. The oil contained low levels of limonene (2.11%), β -flandrene (2.97%), terpinene (1%), m-cymene (1.39%) and β -ocimene (1%) [45]. Similar results were reported that α -pinene (27.27%), β -pinene (43.78%) and β -myrcene (3.37%) were the three main components of barijeh oleoresin. In another study, α -pinene, β -pinene, linalool, α -terpinolene, delta-3-carne and terpinolene were introduced as the most important components of oleoresin Barijah [7,46]. This difference in results may be due to factors such as geographical origin, harvesting time and extraction method of oleoresin [2,6,9,10].

Table 2. Chemical composition of *F. Gummosa* oleoresin by GC-MS Analysis.

Compound	Retention time (min)	Composition (%)
α -thujene	3.603	10.49
α -pinene	4.058	7.53
β -Pinene	4.886	40.27
β -Cymene	5.049	8.21
Cylcofenchene	5.497	11.93
m-Cymene	5.837	1.39
D-limonene	5.938	2.11
β -Phellandrene	5.979	2.97
Trans- β -Ocimene	6.054	0.92
Terpinene	7.255	0.9
α -Cyclogeraniol	8.294	2.22
α -Terpinyl acetate	13.99	1.65
Cadinene	18.144	1.49
Cadina-3,9-diene	18.261	1.69
Junenol	19.787	1.68
Guaiol	20.127	1.44
Cadinol	21.152	2.29
Eudesmol	21.450	4.33
Bulnesol	21.674	2.61
Guaiac acetate	22.740	0.69

3.4. Chemical Structure of Oleoresin

Infrared spectroscopy of oleoresin obtained under extraction conditions is given in Figure 2. FTIR was performed to determine structural information about functional groups and orientation of groups in *F. gummosa* oleoresin. A broad band in the region of 3400 cm⁻¹ represents the stretching vibration of the hydroxyl group (O-H). A similar result was reported for the FTIR spectrum of pomegranate peel pectin [47]. The absorption peak of O-H stretching vibrations was found at 3449 cm⁻¹. A small band was found in the region of 2806 cm⁻¹, indicating the C-H absorption, which includes stretching and bending vibrations of CH, CH₂ and CH₃. It has been reported that the peaks at 2800 cm⁻¹ and 1320 cm⁻¹ are related to CH stretching vibrations of CH₂ groups [48]. In addition, a small band around 2637 cm⁻¹ for oleoresin barijeh indicates the presence of an

aliphatic C-H bond. This C-H absorption and aliphatic C-H bond can be due to methyl ester groups (OCH₃). In addition, two peaks between 1678 and 1460 cm⁻¹ were identified, which are respectively the characteristics of a carbonyl ester group (C=O) and a non-esterified carboxylate ion (COO⁻) [49]. Prominent bands were also detected in the range between 1300 and 1000 cm⁻¹ attributed to C-O stretching in C-O-C and C-O-H. It can be expected due to the common presence of pyranose ring in oleoresin, which are connected to each other through C-O-C glycosidic bonds and C-O-H side group bonds. As noted by Yang et al. [47], the significant absorption band located at 1677 cm⁻¹ was assigned to the C-O stretching vibration of the carbonyl ester, and the absorption band around 1677 cm⁻¹ to the stretching vibration of the unmethylated carboxyl in skin pectin. Pomegranate was shown. [47]. In addition, strong absorption peaks between 1149 and

1018 cm^{-1} indicated the potential presence of pyranose ring. The absorption bands in the range of 1300 and 1450 cm^{-1} for both upper and lower methyl groups were assigned to CH_3 corresponding to asymmetric stretching vibrations, while the bands around 1020 cm^{-1}

were assigned to the saccharide (C-O-C) structure. The IR spectrum for DES (Figure 2) was also determined to check for any residual DES in the extracted oleoresin. The results showed that the IR spectrum of DES was not found in the IR spectrum of oleoresin.

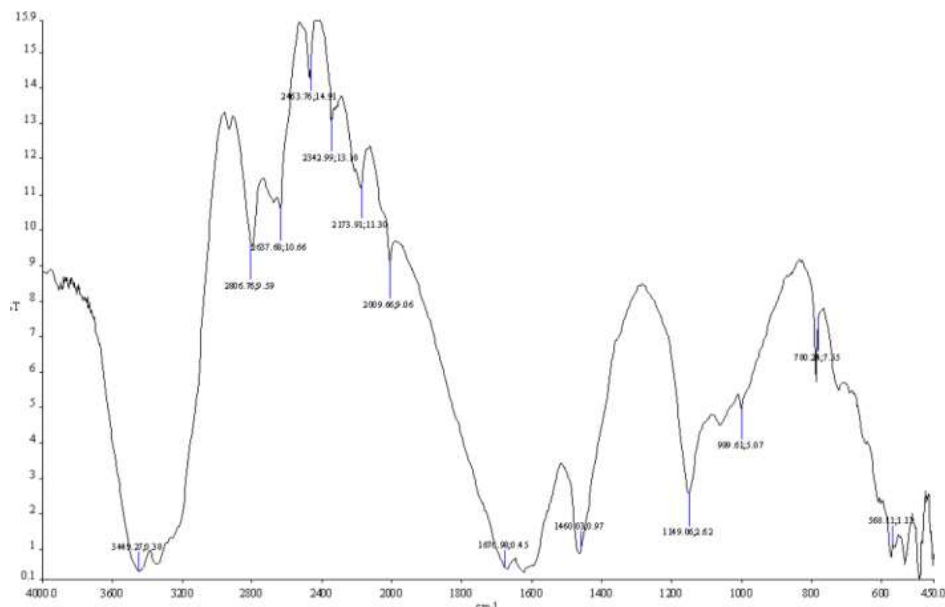
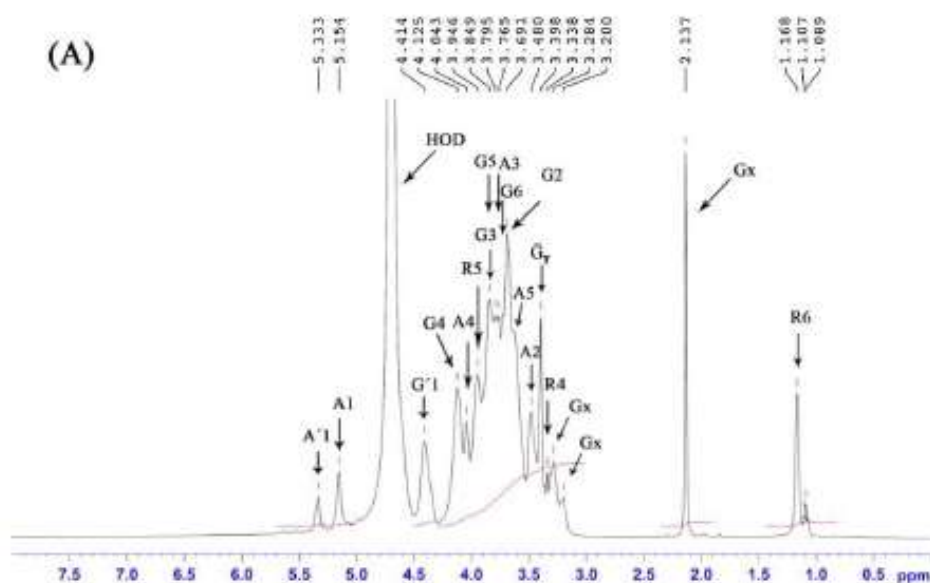


Fig. 2. Structural characterization of *F. gummsa* oleoresin through infrared spectroscopy.

3.5. NMR spectroscopy

^1H NMR and ^{13}C NMR spectra are given in Figure 3. It is clear from the figure that the signals related to anomeric carbon are in the range of 100 to 110 ppm for ^{13}C NMR and 2.4–4.5 ppm for ^1H NMR. The peak in the region of 4.3 to

4.5 ppm in ^1H NMR includes two anomeric signals of β -Gal, which can be followed in the respective spectra. Correlation of carbon signals at 102.57 ppm and 102.9 ppm with proton signals apparently at 4.3 to 4.5 ppm corresponding to $\beta \rightarrow 3,4$ and $\rightarrow 3,4,6$ anomeric carbons. -D-Galp are.



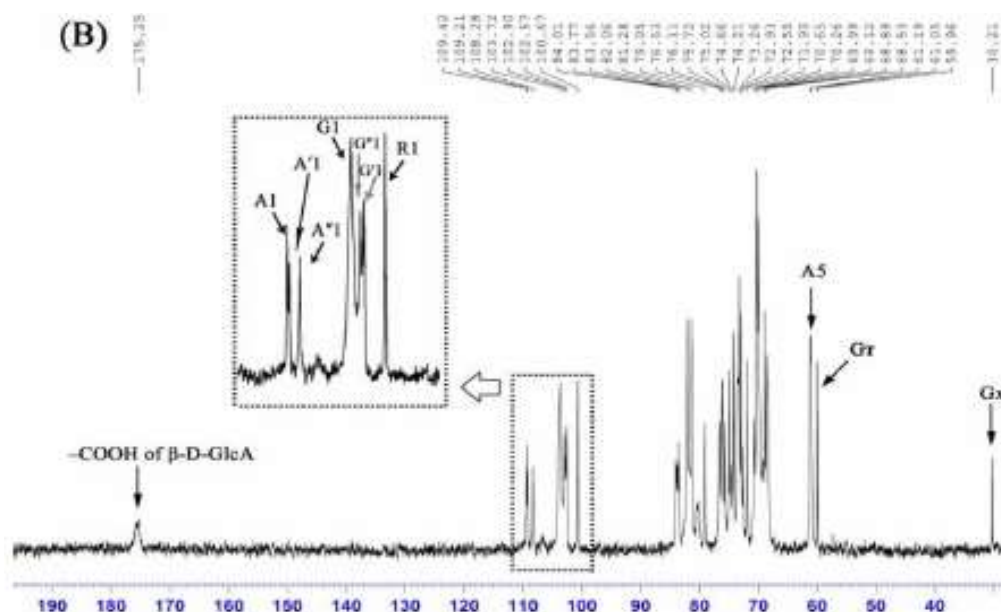


Fig 3. ^1H NMR (A) and ^{13}C NMR spectra of *F.gummsa* oleoresin. Analyses were recorded at 50 g/L in D_2O .

3.6. X-Ray analysis

The XRD pattern of barijeh elorzein showed a small sharp peak at 2θ 17.39 and a broad amorphous region (Figure 4). The crystallinity index was calculated as 15.74%, therefore, the oleoresin sample has a semi-crystalline

microstructure with an amorphous nature. The researchers showed that the crystallization of almond gum is related to the water solubility of each gum fraction. The authors reported the crystallinity index of water-insoluble gum, water-soluble gum, and complete gum as 33.36, 24.27, and 26.46%, respectively [50].

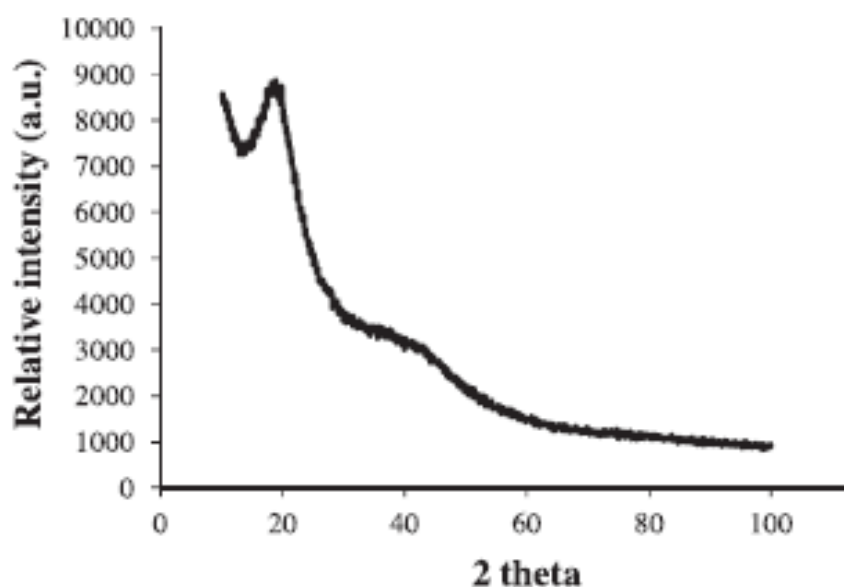


Fig. 4. X-ray diffraction pattern of *F.gummsa* Oleoresin.

3.7. Thermal properties of Oleoresin

The TGA thermogram of barija oleoresin is given in Figure 5A. Heat treatment caused weight loss of oleoresin in two main stages: first at temperatures below 200 $^{\circ}\text{C}$, due to dewatering and second at temperatures above 200 $^{\circ}\text{C}$ due to resin degradation (line A in Figure 5A). In addition, the DTG curve

corresponding to the differential weight loss shows the decomposition rate (line B in Figure 5A). From this point of view, the peak weight loss showed a more intense (about 90.4% weight loss) related to the main thermal degradation, which was related to calcination. Our data were in accordance with the previous findings about gum acacia, which defined temperatures below and above 200 degrees

Celsius as the main areas of weight loss phenomenon [51]. Rao and Mote showed temperatures below 100°C and above 252°C as two distinct weight loss of acacia gum and cashew gum [52]. Fadavi et al. (2014) found that 40-140 °C is related to dehydration and 250-300 °C for the decomposition of Zedo gum [53].

DSC thermogram confirmed the result obtained from TGA analysis (Figure 5). The heating current started to increase gently as the

temperature increased up to 20 °C and then reached its highest level at about 110 °C. The endothermic peak at 110°C is related to water, the exothermic peak observed in the range of 225°C to 331°C is due to dehydration, polymerization and pyrolysis [54]. No Tg was detected due to overlap with the endothermic peak. Some parameters such as particle size, moisture content and the nature of gum are known to be effective on the DSC pattern according to their functional groups [54-52].

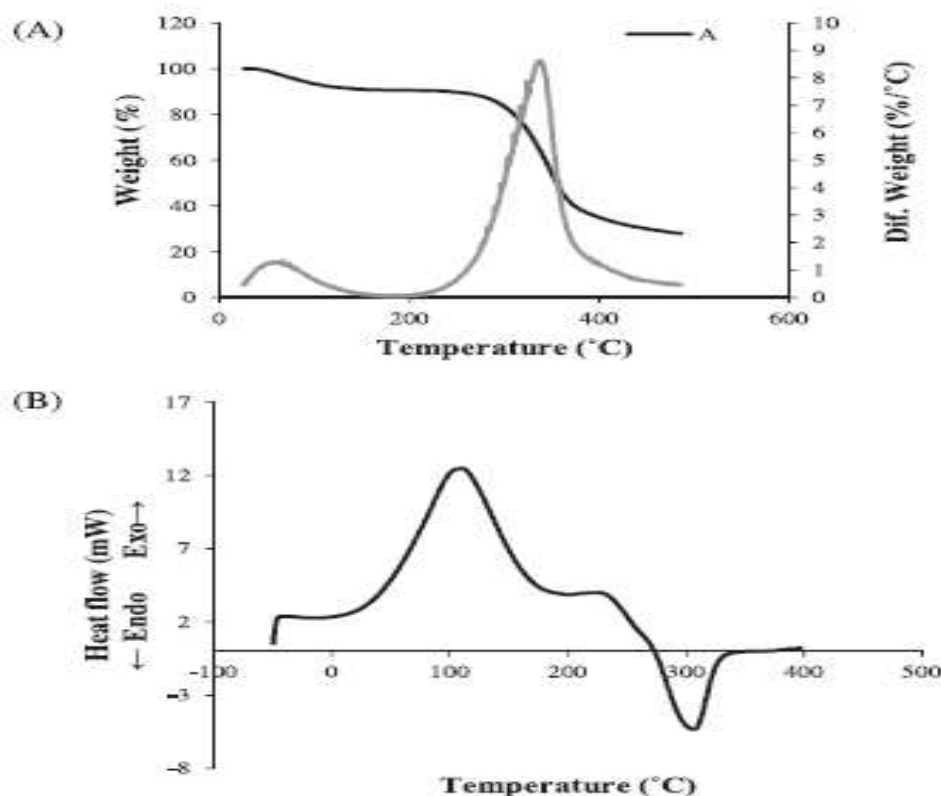


Fig. 5. Thermal behavior of *F.gummsa* Oleoresin: (A) TGA (A line) and DTG (B line) thermogram; (B) DSC thermogram.

3.8. Rheological properties of Oleoresin

The flow behavior of barijeh oleoresin at the shear rate of 10 to 160 s is shown in Figure 6. As it can be seen, with the increase of the cutting degree, the shear stress increased in a non-linear manner, which confirms its non-Newtonian behavior. Examining the changes of apparent viscosity in the range of the studied shear degree revealed that the non-Newtonian behavior was of the thinning type with shear, so that the apparent viscosity decreased with the increase of the shear degree. It should be noted that at high shear rates (200 to 300 s), the apparent viscosity of barijeh oleoresin was almost independent of the shear rate and was similar to Newtonian behavior (data not shown). The results of the studies indicate that

the occurrence of pseudo-plastic behavior of thinning with cutting is due to the occurrence of their flocculation [55-56]. Therefore, their apparent viscosity decreases rapidly due to the breakdown of droplet accumulations due to the application of stress, and gradually when the particles are placed in line with the cutting force, it reaches a constant level, and further increasing the cutting speed does not have much effect. does not have on it The main factor preventing the droplets from approaching and joining together in glycolated oleoresin is the steric repulsion that its molecules create after being absorbed on the surface of the cells. The interesting thing to note about apparent viscosity is its lower numerical value. While it was expected that the covalent binding of oleoresin would increase the viscosity. In most

of the available reports, the increase in the viscosity of the environment has been emphasized [55, 57]. The explanation provided in this regard is that the binding of oleoresin to the biopolymer and the opening of its structure increases the surface hydrophilicity and hydrodynamic radius, which ultimately leads to an increase in the degree of hydration and viscosity [58].

The parameters of flow behavior index (n) and consistency coefficient (k), which were calculated based on power law for oleoresin, were estimated to be 0.246 ± 0.008 and 125.22 ± 0.006 , respectively. The determination coefficient of the model was high ($R^2 = 0.99$),

which indicates the appropriateness of the model used to fit the flow behavior data. The increase in consistency coefficient in this sample indicates the increase in viscosity despite the increase in droplet size; which confirms the connection of cells by considering the thinning behavior with cutting. These observations have also been reported by other researchers and the increase in viscosity depending on the type of protein and carbohydrate used has been attributed to the deficient interconnection or cross-bridge, which are a sign of phase separation on a microscopic scale and the instability of the emulsion system [56, 59].

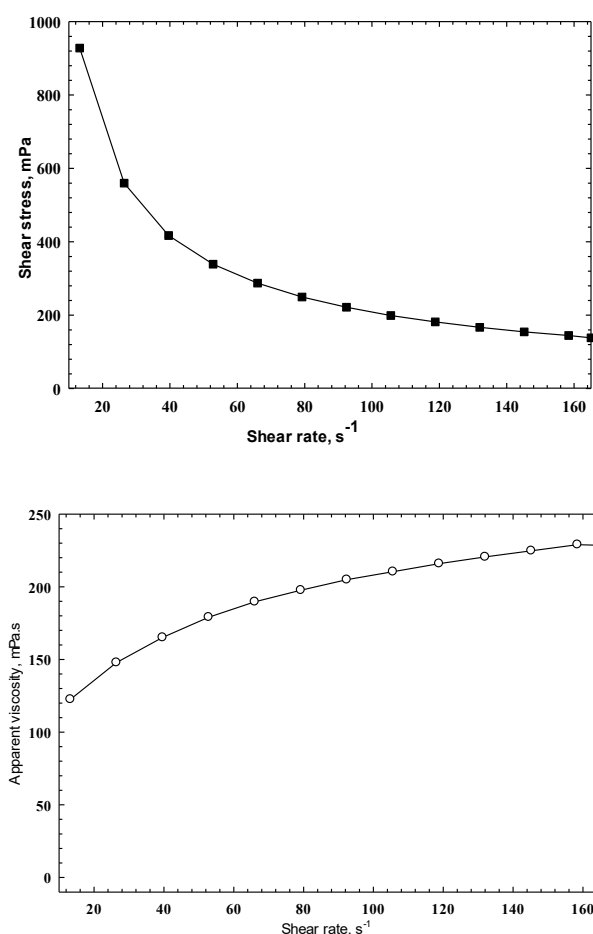


Fig. 6. Rheological behavior of *F.gummsa* Oleoresin.

4. Conclusion

The use of DES is an effective extraction medium for the extraction of barijeh oleoresin. The aim of this work is to compare the natural deep eutectic solvents in the extraction of *Ferula gummosa* (*Ferula gummosa*) and determine its chemical, structural, thermal and rheological properties. Six eutectic solvent mixtures including choline chloride/urea, acetic

acid, lactic acid, formic acid, formamide and glycerol in ratios of 2:1 and 3:1 were evaluated. The highest yield was obtained for choline chloride/formic acid, choline chloride/formamide. The main components of oleoresin were β -pinene (40.27%), silcophenone (11.93%) and alpha-pinene (7.53%), which was determined by gas chromatography-mass spectrometry. Gum was mainly composed of carbohydrates (67.39% by

weight). The polysaccharide consisted of a main backbone of (1 → 3)-β-D-galactan branched mainly from O-6 but also from O-4 and O-4,6. The X-ray diffraction pattern showed a semi-crystalline microstructure. The thermal behavior of the gum was evaluated by thermal analysis (TGA) and differential scanning calorimetry (DSC) showed temperatures below and above 200 °C as the dominant weight loss regions. The rheological behavior of oleoresin was non-Newtonian behavior of shear thinning type, which was well fitted by the power law model. Studying the chemical structure by spectrometry showed that no solvent remained in oleoresin. Therefore, barijeh oleoresin can be used as a promising natural medicinal substance extracted with eutectic solvents, while these eutectic solvents can be used as a green method for many herbal compounds.

5. References

- [1] Mortazaienezhad, F.; Sadeghian, M.M. Investigation of Compounds from Galbanum (Ferula Gummosa) Boiss. *Asian J. Plant Sci.* **2006**.
- [2] NAJAF NAJAFI, M.; Arianmehr, A.; Sani, A.M. Preparation of Barije (Ferula Gummosa) Essential Oil-loaded Liposomes and Evaluation of Physical and Antibacterial Effect on Escherichia Coli O157: H7. *J. Food Prot.* **2020**, *83*, 511–517.
- [3] Talebi Kouyakh, E.; Naghavi, M.R.; Alayhs, M. Study of the Essential Oil Variation of Ferula Gummosa Samples from Iran. *Chem. Nat. Compd.* **2008**, *44*, 124–126.
- [4] Abedi, D.; Jalali, M.; Sadeghi, N. Composition and Antimicrobial Activity of Oleogumresin of Ferula Gumosa Bioss. Essential Oil Using Alamar Blue™. *Res. Pharm. Sci.* **2009**, *3*, 41–45.
- [5] Jalali, H.T.; Petronilho, S.; Villaverde, J.J.; Coimbra, M.A.; Domingues, M.R.M.; Ebrahimian, Z.J.; Silvestre, A.J.D.; Rocha, S.M. Assessment of the Sesquiterpenic Profile of Ferula Gummosa Oleo-Gum-Resin (Galbanum) from Iran. Contributes to Its Valuation as a Potential Source of Sesquiterpenic Compounds. *Ind. Crops Prod.* **2013**, *44*, 185–191.
- [6] Jalali, H.T.; Petronilho, S.; Villaverde, J.J.; Coimbra, M.A.; Domingues, M.R.M.; Ebrahimian, Z.J.; Silvestre, A.J.D.; Rocha, S.M. Deeper Insight into the Monoterpenic Composition of Ferula Gummosa Oleo-Gum-Resin from Iran. *Ind. Crops Prod.* **2012**, *36*, 500–507.
- [7] Ghasemi, Y.; Faridi, P.; Mehregan, I.; Mohagheghzadeh, A. Ferula Gummosa Fruits: An Aromatic Antimicrobial Agent. *Chem. Nat. Compd.* **2005**, *41*, 311–314.
- [8] Ghannadi, A.; Amree, S. Volatile Oil Constituents of Ferula Gummosa Boiss. from Kashan, Iran. *J. Essent. Oil Res.* **2002**, *14*, 420–421.
- [9] Jalali, H.T.; Ebrahimian, Z.J.; Evtuguin, D. V.; Neto, C.P. Chemical Composition of Oleo-Gum-Resin from Ferula Gummosa. *Ind. Crops Prod.* **2011**, *33*, 549–553.
- [10] Jeong, K.M.; Han, S.Y.; Kim, E.M.; Jin, Y.; Lee, J. Deep Eutectic Solvent-Based Valorization of Spent Coffee Grounds. *Food Chem.* **2018**, *255*, 357–364.
- [11] Barbieri, J.B.; Goltz, C.; Cavaleiro, F.B.; Toci, A.T.; Igarashi-Mafra, L.; Mafra, M.R. Deep Eutectic Solvents Applied in the Extraction and Stabilization of Rosemary (Rosmarinus Officinalis L.) Phenolic Compounds. *Ind. Crops Prod.* **2020**, *144*, 112049.
- [12] Ruesgas-Ramón, M.; Figueroa-Espinoza, M.C.; Durand, E. Application of Deep Eutectic Solvents (DES) for Phenolic Compounds Extraction: Overview, Challenges, and Opportunities. *J. Agric. Food Chem.* **2017**, *65*, 3591–3601.
- [13] Wang, M.; Wang, J.; Zhou, Y.; Zhang, M.; Xia, Q.; Bi, W.; Chen, D.D.Y. Ecofriendly Mechanochemical Extraction of Bioactive Compounds from Plants with Deep Eutectic Solvents. *ACS Sustain. Chem. Eng.* **2017**, *5*, 6297–6303.
- [14] Cao, J.; Yang, M.; Cao, F.; Wang, J.; Su, E. Well-Designed Hydrophobic Deep Eutectic Solvents as Green and Efficient Media for the Extraction of Artemisinin from Artemisia Annu Leaves. *ACS Sustain. Chem. Eng.* **2017**, *5*, 3270–3278.
- [15] Machmudah, S.; Lestari, S.D.; Kanda, H.; Winardi, S.; Goto, M. Subcritical Water Extraction Enhancement by Adding Deep Eutectic Solvent for Extracting Xanthone from Mangosteen Pericarps. *J. Supercrit. Fluids* **2018**, *133*, 615–624.
- [16] Abbott, A.P.; Boothby, D.; Capper, G.; Davies, D.L.; Rasheed, R.K. Deep Eutectic Solvents Formed between Choline Chloride and Carboxylic Acids: Versatile Alternatives to Ionic Liquids. *J. Am. Chem. Soc.* **2004**, *126*, 9142–9147.
- [17] Syakfanaya, A.M.; Saputri, F.C.; Mun'im, A. Simultaneously Extraction of Caffeine and Chlorogenic Acid from Coffea Canephora Bean

Using Natural Deep Eutectic Solvent-Based Ultrasonic Assisted Extraction. *Pharmacogn. J.* **2019**, *11*.

[18] Paiva, A.; Craveiro, R.; Aroso, I.; Martins, M.; Reis, R.L.; Duarte, A.R.C. Natural Deep Eutectic Solvents—solvents for the 21st Century. *ACS Sustain. Chem. Eng.* **2014**, *2*, 1063–1071.

[19] Dai, Y.; Witkamp, G.-J.; Verpoorte, R.; Choi, Y.H. Tailoring Properties of Natural Deep Eutectic Solvents with Water to Facilitate Their Applications. *Food Chem.* **2015**, *187*, 14–19.

[20] Shahbaz, K.; Baroutian, S.; Mjalli, F.S.; Hashim, M.A.; AlNashef, I.M. Densities of Ammonium and Phosphonium Based Deep Eutectic Solvents: Prediction Using Artificial Intelligence and Group Contribution Techniques. *Thermochim. Acta* **2012**, *527*, 59–66.

[21] Maugeri, Z.; de María, P.D. Novel Choline-Chloride-Based Deep-Eutectic-Solvents with Renewable Hydrogen Bond Donors: Levulinic Acid and Sugar-Based Polyols. *Rsc Adv.* **2012**, *2*, 421–425.

[22] Ribeiro, B.D.; Coelho, M.A.Z.; Marrucho, I.M. Extraction of Saponins from Sisal (Agave Sisalana) and Juá (Ziziphus Joazeiro) with Cholinium-Based Ionic Liquids and Deep Eutectic Solvents. *Eur. Food Res. Technol.* **2013**, *237*, 965–975.

[23] Yuniarti, E.; Saputri, F.C.; Munâ, A. Application of the Natural Deep Eutectic Solvent Choline Chloride-Sorbitol to Extract Chlorogenic Acid and Caffeine from Green Coffee Beans (Coffea Canephora). *J. Appl. Pharm. Sci.* **2019**, *9*, 82–90.

[24] Ahmad, I.; Pertiwi, A.S.; Kembaren, Y.H.; Rahman, A.; Munâ, A. Application of Natural Deep Eutectic Solvent-Based Ultrasonic Assisted Extraction of Total Polyphenolic and Caffeine Content from Coffe Beans (Coffea Beans L.) for Instant Food Products. *J. Appl. Pharm. Sci.* **2018**, *8*, 138–143.

[25] Nadia, J.; Shahbaz, K.; Ismail, M.; Farid, M.M. Approach for Polygodial Extraction from Pseudowintera Colorata (Horopito) Leaves Using Deep Eutectic Solvents. *ACS Sustain. Chem. Eng.* **2018**, *6*, 862–871.

[26] Cao, J.; Chen, L.; Li, M.; Cao, F.; Zhao, L.; Su, E. Efficient Extraction of Proanthocyanidin from Ginkgo Biloba Leaves Employing Rationally Designed Deep Eutectic Solvent-Water Mixture and Evaluation of the Antioxidant Activity. *J. Pharm. Biomed. Anal.* **2018**, *158*, 317–326.

[27] Křížek, T.; Bursová, M.; Horsley, R.;

Kuchař, M.; Tůma, P.; Čabala, R.; Hložek, T. Menthol-Based Hydrophobic Deep Eutectic Solvents: Towards Greener and Efficient Extraction of Phytocannabinoids. *J. Clean. Prod.* **2018**, *193*, 391–396.

[28] Athanasiadis, V.; Grigorakis, S.; Lalas, S.; Makris, D.P. Highly Efficient Extraction of Antioxidant Polyphenols from Olea Europaea Leaves Using an Eco-Friendly Glycerol/glycine Deep Eutectic Solvent. *Waste and Biomass Valorization* **2018**, *9*, 1985–1992.

[29] Liew, S.Q.; Ngoh, G.C.; Yusoff, R.; Teoh, W.H. Acid and Deep Eutectic Solvent (DES) Extraction of Pectin from Pomelo (Citrus Grandis (L.) Osbeck) Peels. *Biocatal. Agric. Biotechnol.* **2018**, *13*, 1–11.

[30] Ma, W.; Row, K.H. Optimized Extraction of Bioactive Compounds from Herba Artemisiae Scopariae with Ionic Liquids and Deep Eutectic Solvents. *J. Liq. Chromatogr. Relat. Technol.* **2017**, *40*, 459–466.

[31] De Faria, E.L.P.; Do Carmo, R.S.; Cláudio, A.F.M.; Freire, C.S.R.; Freire, M.G.; Silvestre, A.J.D. Deep Eutectic Solvents as Efficient Media for the Extraction and Recovery of Cynaropicrin from Cynara Cardunculus L. Leaves. *Int. J. Mol. Sci.* **2017**, *18*, 2276.

[32] Dai, Y.; Verpoorte, R.; Choi, Y.H. Natural Deep Eutectic Solvents Providing Enhanced Stability of Natural Colorants from Safflower (Carthamus Tinctorius). *Food Chem.* **2014**, *159*, 116–121.

[33] Huang, Y.; Feng, F.; Jiang, J.; Qiao, Y.; Wu, T.; Voglmeir, J.; Chen, Z.-G. Green and Efficient Extraction of Rutin from Tartary Buckwheat Hull by Using Natural Deep Eutectic Solvents. *Food Chem.* **2017**, *221*, 1400–1405.

[34] Wang, T.; Jiao, J.; Gai, Q.-Y.; Wang, P.; Guo, N.; Niu, L.-L.; Fu, Y.-J. Enhanced and Green Extraction Polyphenols and Furanocoumarins from Fig (Ficus Carica L.) Leaves Using Deep Eutectic Solvents. *J. Pharm. Biomed. Anal.* **2017**, *145*, 339–345.

[35] Zhao, B.-Y.; Xu, P.; Yang, F.-X.; Wu, H.; Zong, M.-H.; Lou, W.-Y. Biocompatible Deep Eutectic Solvents Based on Choline Chloride: Characterization and Application to the Extraction of Rutin from Sophora Japonica. *ACS Sustain. Chem. Eng.* **2015**, *3*, 2746–2755.

[36] Wei, Z.; Qi, X.; Li, T.; Luo, M.; Wang, W.; Zu, Y.; Fu, Y. Application of Natural Deep Eutectic Solvents for Extraction and Determination of

Phenolics in Cajanus Cajan Leaves by Ultra Performance Liquid Chromatography. *Sep. Purif. Technol.* **2015**, 149, 237–244.

[37] Abbott AP, Boothby D, Capper G, Davies DL, Rasheed RK. Deep eutectic solvents formed between choline chloride and carboxylic acids: versatile alternatives to ionic liquids. *J Am Chem Soc. ACS Publications*; **2004**;126:9142–7.

[38] Sandra P, Bicchi C. Capillary gas chromatography in essential oil analysis. **1987**.

[39] Fernández AG, Adams MR, Fernández-Díez MJ. Table olives: production and processing. *Springer Science & Business Media*; **1997**.

[40] Rafe A, Razavi SMA. Effect of thermal treatment on chemical structure of β -lactoglobulin and basil seed gum mixture at different states by ATR-FTIR spectroscopy. *Int J Food Prop.* **2015**;18:2652–64.

[41] Shahbazi M, Rajabzadeh G, Rafe A, Ettelaie R, Ahmadi SJ. The physico-mechanical and structural characteristics of blend film of poly (vinyl alcohol) with biodegradable polymers as affected by disorder-to-order conformational transition. *Food Hydrocoll.* **2016**;60.

[42] Chen W, Xue Z, Wang J, Jiang J, Zhao X, Mu T. Investigation on the thermal stability of deep eutectic solvents. *Acta Phys Chim Sin.* **2018**;34:904–11.

[43] Shafie MH, Yusof R, Gan C-Y. Deep eutectic solvents (DES) mediated extraction of pectin from Averrhoa bilimbi: Optimization and characterization studies. *Carbohydr Polym.* **2019**;216:303–11.

[44] Wang W, Li X, Bao X, Gao L, Tao Y. Extraction of polysaccharides from black mulberry fruit and their effect on enhancing antioxidant activity. *Int J Biol Macromol.* **2018**;120:1420–9.

[45] Rios J-L, Recio MC. Medicinal plants and antimicrobial activity. *J Ethnopharmacol. Elsevier*; **2005**;100:80–4.

[46] Eftekhari F, Yousefzadi M, Borhani K. Antibacterial activity of the essential oil from Ferula gummosa seed. *Fitoterapia. Elsevier*; **2004**;75:758–9.

[47] Yang X, Nisar T, Hou Y, Gou X, Sun L, Guo Y. Pomegranate peel pectin can be used as an effective emulsifier. *Food Hydrocoll. Elsevier*; **2018**;85:30–8.

[48] He L, Zhang X, Xu H, Xu C, Yuan F, Knez Ž, et al. Subcritical water extraction of phenolic compounds from pomegranate (*Punica granatum* L.) seed residues and investigation into their antioxidant

activities with HPLC–ABTS+ assay. *Food Bioprod Process. Elsevier*; **2012**;90:215–23.

[49] Manrique GD, Lajolo FM. FT-IR spectroscopy as a tool for measuring degree of methyl esterification in pectins isolated from ripening papaya fruit. *Postharvest Biol Technol. Elsevier*; **2002**;25:99–107.

[50] Saeidy S, Nasirpour A, Keramat J, Desbrières J, Le Cerf D, Pierre G, Delattre C, Laroche C, De Baynast H, Ursu AV, Marcati A. Structural characterization and thermal behavior of a gum extracted from Ferula assa foetida L. *Carbohydrate polymers.* **2018**;181:426–32.

[51] Cozic C, Picton L, Garda MR, Marlhoux F, Le Cerf D. Analysis of arabic gum: Study of degradation and water desorption processes. *Food Hydrocolloids.* **2009**;23(7):1930–4.

[52] Mothé CG, Rao MA. Thermal behavior of gum arabic in comparison with cashew gum. *Thermochimica acta.* **2000**;357:9–13.

[53] Fadavi G, Mohammadifar MA, Zargarran A, Mortazavian AM, Komeili R. Composition and physicochemical properties of Zedo gum exudates from Amygdalus scoparia. *Carbohydrate polymers.* **2014**;101:1074–80.

[54] Zohuriaan MJ, Shokrolahi FJ. Thermal studies on natural and modified gums. *Polymer testing.* **2004**;23(5):575–9.

[55] Xu L, Dong M, Gong H, Sun M, Li Y. Effects of inorganic cations on the rheology of aqueous welan, xanthan, gellan solutions and their mixtures. *Carbohydrate polymers.* **2015**;121:147–54.

[56] Diftis NG, Biliaderis CG, Kiosseoglou VD. Rheological properties and stability of model salad dressing emulsions prepared with a dry-heated soybean protein isolate–dextran mixture. *Food hydrocolloids.* **2005**;19(6):1025–31.

[57] Paraman I, Hettiarachchy NS, Schaefer C, Beck MI. Hydrophobicity, solubility, and emulsifying properties of enzyme-modified rice endosperm protein. *Cereal chemistry.* **2007**;84(4):343–9.

[58] Baniel A, Caer D, Colas B, Gueguen J. Functional properties of glycosylated derivatives of the 11S storage protein from pea (*Pisum sativum* L.). *Journal of Agricultural and food Chemistry.* **1992**;40(2):200–5.

[59] Benichou A, Aserin A, Garti N. W/O/W double emulsions stabilized with WPI–polysaccharide complexes. *Colloids and Surfaces A: Physicochemical and Engineering Aspects.* **2007**;294(1–3):20–32.



بررسی خواص الثورزین صمغ باریجه استخراج شده به روش حلال‌های عمیق یوتکتیک

جواد رادمرد^۱، علی محمدی ثانی کاخکی^{۲*}، اکرم آریانفر^۲ و بهروز محمودزاده وزیری^۳

۱- دانشجوی دکتری، گروه علوم و صنایع غذایی، واحد قوچان، دانشگاه آزاد اسلامی، قوچان، ایران

۲- گروه علوم و صنایع غذایی، واحد قوچان، دانشگاه آزاد اسلامی، قوچان، ایران

۳- گروه مهندسی شیمی، واحد قوچان، دانشگاه آزاد اسلامی، قوچان، ایران

۴- گروه مهندسی شیمی، واحد مشهد، دانشگاه آزاد اسلامی، مشهد، ایران

اطلاعات مقاله

چکیده

تاریخ های مقاله :

تاریخ دریافت: ۱۴۰۲/۰۷/۱۲

تاریخ پذیرش: ۱۴۰۳/۰۲/۰۴

کلمات کلیدی:

استخراج،

الثورزین،

باریجه،

خواص عملکردی-ساختمانی.

DOI: 10.48311/fsct.2025.83974.0.

* مسئول مکاتبات:

Mohamadisani@yahoo.com

حلال‌های یوتکتیک عمیق در استخراج متابولیت‌های گیاهی مزایای زیادی مانند سمیت کم، زیست‌تخریب‌پذیری، هزینه کم و سهولت آماده‌سازی نسبت به روش‌های مرسوم یافته‌اند. هدف این کار مقایسه حلال‌های یوتکتیک عمیق طبیعی در استخراج الثورزین باریجه (*Ferula gummosa*) و تعیین خواص شیمیایی، ساختمانی، ساختاری، حرارتی و رئولوژیکی آن است. شش مخلوط حلال یوتکتیک شامل کولین کلرید/اوره، اسید استیک، اسید لاکتیک، اسید فرمیک، فرمامید و گلیسرول در نسبت‌های ۲:۱ و ۳:۱ مورد ارزیابی قرار گرفت. بیشترین بازده برای کولین کلرید/اسید فرمیک، کولین کلرید/فرمامید به دست آمد. اجزای اصلی اولئورزین β -پنین (۴۰٪/۲۷٪)، سیلکوفنشن (۱۱/۹۳٪) و آلفا پنین (۷/۵۳٪) بودند که توسط کروماتوگرافی گازی-طیف سنجی جرمی مشخص شد. صمغ عمدتاً از کربوهیدرات‌ها (۶۷/۳۹٪ وزنی) تشکیل شده بود. پلی ساکارید شامل یک ستون اصلی (۱ \rightarrow ۳) β -D-گالاکتان بود که عمدتاً از O-6 و همچنین از O-4 و O-4+6 منشعب می‌شد. الگوی پراش اشعه ایکس یک ریزساختار نیمه کریستالی را نشان داد. رفتار حرارتی صمغ با تجزیه و تحلیل حرارتی (TGA) ارزیابی شد و کالریتری روبشی تفاضلی (DSC) دماهای زیر و بالای ۲۰۰ درجه سانتیگراد را به عنوان مناطق غالب کاهش وزن نشان داد. رفتار رئولوژیکی الثورزین رفتار غیرنیوتنی از نوع رقیق شونده با برش بود که با مدل قانون توان به خوبی برازش داده شد. مطالعه ساختار شیمیایی توسط طیف سنجی نشان داد که هیچ حلالی در الثورزین باقی نمانده است. بنابراین، الثورزین باریجه را می‌توان به عنوان یک ماده دارویی طبیعی نویدبخش استخراج شده با حلال‌های یوتکتیک مورد استفاده قرار داد، ضمن آنکه این حلال‌های یوتکتیک به عنوان روشی سبز قابلیت استفاده برای بسیاری از ترکیبات گیاهی را دارند.